Biochimica et Biophysica Acta 1840 (2014) 605–614

Contents lists available at ScienceDirect

Biochimica et Biophysica Acta

journal homepage: www.elsevier.com/locate/bbagen

Decreased solute adsorption onto cracked surfaces of mechanically injured articular cartilage: Towards the design of cartilage-specific functional contrast agents

Mohammad Moeini, Sarah G.A. Decker, Hooi Chuan Chin, Yousef Shafieyan, Derek H. Rosenzweig, Thomas M. Quinn *

Department of Chemical Engineering, McGill University, Montreal, QC, Canada

ARTICLE INFO

Article history:
Received 21 June 2013
Received in revised form 5 October 2013
Accepted 14 October 2013
Available online 18 October 2013

Keywords:
Articular cartilage
Contrast agent
Dextrans
FITC
Injury
Solute adsorption

ABSTRACT

Background: Currently available methods for contrast agent-based magnetic resonance imaging (MRI) and computed tomography (CT) of articular cartilage can only detect cartilage degradation after biochemical changes have occurred within the tissue volume. Differential adsorption of solutes to damaged and intact surfaces of cartilage may be used as a potential mechanism for detection of injuries before biochemical changes in the tissue volume occur.
Methods: Adsorption of four fluorescent macromolecules to surfaces of injured and sliced cartilage explants was studied. Solutes included native dextran, dextrans modified with aldehyde groups or a chondroitin sulfate (CS)-binding peptide and the peptide alone.
Results: Adsorption of solutes to fissures was significantly less than to intact surfaces of injured and sliced explants. Moreover, solute adsorption at intact surfaces of injured and sliced explants was less reversible than at surfaces of uninjured explants. Modification of dextrans with aldehyde or the peptide enhanced adsorption with the same level of differential adsorption to cracked and intact surfaces. However, aldehyde–dextran exhibited irreversible adsorption. Equilibration of explants in solutes did not decrease the viability of chondrocytes.
Conclusions and general significance: Studied solutes showed promising potential for detection of surface injuries based on differential interactions with cracked and intact surfaces. Additionally, altered adsorption properties at surfaces of damaged cartilage which visually look healthy can be used to detect micro-damage or biochemical changes in these regions. Studied solutes can be used in in vivo fluorescence imaging methods or conjugated with MRI or CT contrast agents to develop functional imaging agents.

1. Introduction

Articular cartilage is a specialized tissue which covers the sliding surfaces of articulating bones to provide a weight-bearing, smooth surface with low friction [1]. This tissue is highly resistant to compression and shear stresses [2]. However, cartilage exhibits limited self-repair capability due to its avascular nature, low cell density and limited chondrocyte proliferation [2,3]. In primary osteoarthritis, biochemical changes within the cartilage volume can occur over time without any prior condition or external event (like tissue injury) [4], eventually leading to structural changes such as surface fibrillation and fissures. On the other hand, surface damage to articular cartilage can lead to gradual biochemical changes over cartilage volume which ultimately lead to tissue breakdown, more severe cracks, and development of secondary osteoarthritis [5,6]. Development of sensitive and noninvasive imaging tools is therefore essential to detect cartilage injuries and surface irregularities immediately after the insult.

Conventional magnetic resonance imaging (MRI) and X-ray computed tomography (CT) [7–9] only provide anatomical information; hence, signs of cartilage degeneration can be detected when tissue has gone through severe structural and compositional changes [10]. As glycosaminoglycan (GAG) loss is an early hallmark of cartilage degradation [11], contrast enhanced imaging methods like delayed Gadolinium-Enhanced MRI of Cartilage (dGEMRIC) [12] and Contrast Enhanced Computed Tomography (CECT) [13] have been developed to detect cartilage degradation based on alterations in GAG content. In these methods, distribution of anionic [12] or cationic [14] contrast agents are assumed to represent the spatial distribution of negatively charged GAGs within the matrix. The limitation of these techniques is that they are able to detect cartilage degradation only after a significant change in GAG content. Recently, alterations in diffusion rates of contrast agents in cartilage have been suggested for assessment of cartilage

* Corresponding author at: Department of Chemical Engineering, McGill University, 3610 University Street, Montreal, QC H3A 0C5, Canada. Tel.: +1 514 398 4494; fax: +1 514 398 6678.
E-mail address: thomas.quinn@mcgill.ca (T.M. Quinn).

0304-4165/$ – see front matter © 2013 Elsevier B.V. All rights reserved.
http://dx.doi.org/10.1016/j.bbagen.2013.10.022

integrity [15,16]. However, it was shown that solute diffusion is affected only in injured explants with biochemical or structural changes in tissue volume, but solute diffusion was not altered in sliced explants [17]. There is therefore a need for developing new imaging approaches which are able to detect cartilage surface injuries and irregularities well before structural or biochemical changes in the whole tissue volume occur.

We have recently reported that a wide range of fluorescent solutes adsorb onto surfaces of cartilage explants [18] and also that small fluorophores adsorb less significantly at surfaces of fissures compared to adjacent intact surfaces of mechanically injured explants [19]. These findings encourage the conjugation of CT, MRI or fluorescence agents to carrier molecules with differential adsorption onto damaged and intact surfaces of cartilage as a potential approach for development of new functional imaging agents based on solute–surface interactions (as opposed to solute interactions with extracellular matrix components within the cartilage volume in currently available contrast agent-based cartilage imaging methods) for early detection of surface injuries and abnormalities. It is also possible to enhance the contrast agent performance or make it more selective by chemical functionalization of the carrier molecule.

In the present study we therefore aimed to extend previous findings on adsorption of small fluorophores at surfaces of injured cartilage [19] to examine differential adsorption of fluorescently labeled native and modified dextrans to cracked and intact surfaces of mechanically injured cartilage. Dextrans are excellent choices for carrier molecules because they are natural, biodegradable and pharmacologically inert and have been widely used in other medical applications [20–27]. In addition, dextrans are available commercially in different molecular weights and have numerous hydroxyl groups that can be easily used for chemical modification or conjugation to imaging agents [22,23]. A relatively big dextran (70 kDa) was used in this study to examine carrier molecules which have limited penetration into the cartilage and interact mostly with its surfaces. It should be noted that limited contrast agent penetration into cartilage matrix can be beneficial in this application (imaging using surface interactions) since this reduces the interfering signals from within the cartilage volume, resulting in more sensitive detection of surface abnormalities. Dextran was modified by introducing either aldehyde groups or a chondroitin sulfate (CS)-binding peptide to its structure to study if the performance of dextran as a carrier molecule will be improved. It has been shown that aldehyde modification enhances molecular binding to cartilage surfaces [28]. On the other hand, chondroitin sulfate is the main GAG in cartilage matrix [29]. The CS-binding peptide alone was also studied. Findings from this study provide insights for potential novel carrier molecule designs for new contrast agents.

2. Methods

2.1. Solutes

Solutes included 70 kDa dextran (Dex), aldehyde–dextran (Dex–CHO) and a chondroitin sulfate (CS)-binding peptide (peptide). Additionally, dextran conjugated with the CS-binding peptide (Dex–peptide) was also included in some experiments. All solutes were labeled with fluorescein isothiocyanate (FITC). FITC was selected as fluorescent label because it has been shown that compared to positively charged fluorophores (tetramethylrhodamine isothiocyanate (TRITC) and carboxytetramethylrhodamine (TAMRA)), negatively charged FITC affects the adsorption of solutes onto cartilage surfaces less significantly [18]. In addition, our previous study [19] showed that TRITC and TAMRA do not exhibit superior sensitivity in distinguishing cracked from intact surfaces compared to FITC. 70 kDa dextran already conjugated with FITC was obtained from Sigma. It was used directly or oxidized by sodium periodate (Sigma) with sodium periodate/glucose unit molar ratio of 1 to obtain FITC conjugated Dex–CHO [30]. A CS-binding peptide (sequence: YKTNFRRYYRF, MW: 2115) conjugated to FITC was obtained from CanPeptide Inc. The amino acid sequence of the peptide was based on a previous study [31]. The same peptide without FITC label (MW: 1613) was obtained from CanPeptide Inc. and was conjugated to FITC labeled Dex–CHO by established protocols [20,32] at peptide/aldehyde molar ratio of 0.09.

2.2. Solute characterization

Absorbance spectra of Dex (0.22 mg/ml) and Dex–CHO (0.16 mg/ml) were obtained using a UV–visible spectrophotometer (Evolution 300, Thermo Scientific) to confirm the aldehyde modification of dextran. The degree of aldehyde modification was determined by hydroxylamine titration assay [33]. Raman spectra of Dex (0.03 mg/ml) and Dex–peptide (0.04 mg/ml) were obtained using a DXR Raman microscope (Thermo Scientific) with 532 nm excitation laser to confirm the presence of peptide in the structure of Dex–peptide.

2.3. Cartilage explants

Visually healthy osteochondral cores, 5 mm in diameter, were drilled from the distal femur of skeletally mature adult bovine knees and their cartilage was trimmed to the 3 mm diameter (Fig. 1A). Trimmed samples were then randomly assigned into three groups (injured, uninjured controls, and sliced positive controls) and incubated in chondrocyte culture medium (high-glucose DMEM; 0.1 mM nonessential amino acids; 10 mM HEPES; 10% fetal bovine serum; and 1% penicillin–streptomycin–amphotericin) (Life Technologies) for 1–2 days until experimental use. All the experiments were performed in a 37 °C, 5% CO_2 environment.

2.4. Mechanical injury and positive control slicing

Osteochondral cores were injured by single radially unconfined axial compression at 0.7 s^{-1} strain rate and 14 MPa peak stress as described previously [34]. For comparison, positive sliced controls were created by slicing the articular surface of uninjured explants to a depth of approximately 200 μm along the diameter using a vibratome (VT1200, Leica Microsystems). Injured and sliced explants were used in experiments within 2 h of injury or slicing.

2.5. Equilibration and desorption baths

Solute adsorption to cartilage surfaces was examined after equilibration with the solute or after equilibration and subsequent desorption processes. Uninjured (control), injured or sliced osteochondral explants were equilibrated with culture medium containing Dex (0.28 mg/ml), Dex–CHO (0.28 mg/ml), Dex–peptide (0.18 mg/ml) or peptide (0.0085 mg/ml) for 20–22 h. For desorption experiments, explants were then removed from equilibration baths, rinsed with blank culture medium and transferred to blank culture medium baths for another 20–22 h. Osteochondral cores from at least three different joints were mixed and 6 explants were used randomly for each solute of each group (uninjured, injured or sliced) for adsorption or desorption experiments. In the case of Dex–peptide, only solute adsorption to surfaces of uninjured ($n = 4$) and injured explants ($n = 6$) after equilibration process was examined.

2.6. Long-term desorption

To examine the reversibility of adsorption and bulk uptake (absorption) of solutes, an independent experiment was performed in which uninjured explants were equilibrated with culture medium containing Dex–CHO (0.28 mg/ml), Dex–peptide (0.18 mg/ml) or peptide (0.0085 mg/ml) for 24 h. Explants were removed from equilibration baths for fluorescence microscopy or they were transferred

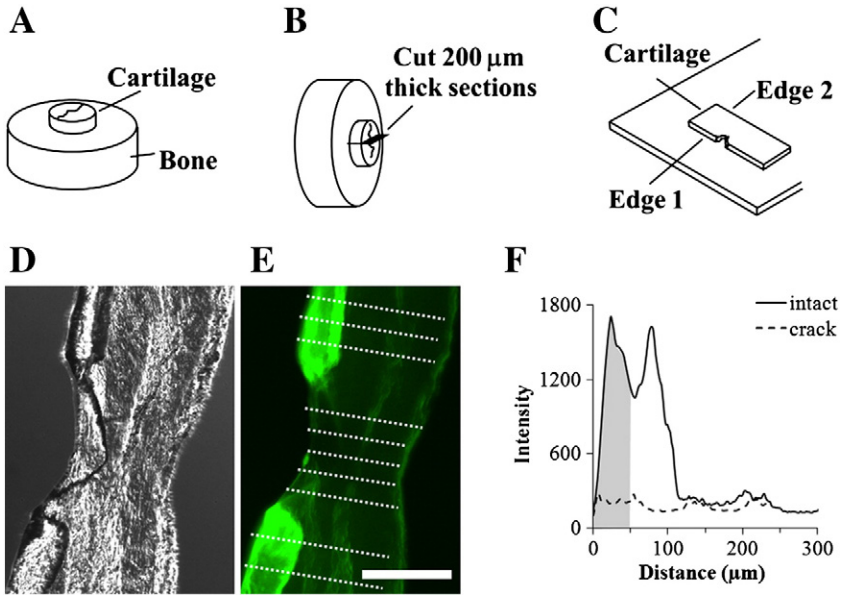

Fig. 1. Osteochondral cores (A) were incubated in equilibration and desorption baths. 200 μm thick sections were then cut through the cartilage depth (B) and mounted on a microscope slide (C) for fluorescence microscopy of articular surface in direct contact with the bath (Edge 1) and the control edge not exposed to any bath (Edge 2). (D) A representative light microscope image of a 200 μm thick section of injured cartilage. (E) Fluorescence microscope image of cartilage section shown in (D) equilibrated with aldehyde–dextran. Fluorescence images were analyzed by taking the mean of five line-scans on intact and cracked regions (E) and calculating the average fluorescence intensity in the first 50 μm of the resulting intensity vs. distance curves (F). Scale bar is 200 μm.

to blank culture medium baths for 2 or 5 days of desorption. During desorption period, explants were rinsed with blank culture medium and were transferred to new blank culture medium baths every 24 h. Osteochondral cores from four different joints were mixed and 3 explants were used randomly for each solute of each group (adsorption, 2 days desorption or 5 days desorption).

2.7. Fluorescence microscopy

Osteochondral explants were removed from equilibration or desorption baths and 200 μm thick sections (three sections per explant) were cut perpendicular to the articular surface using a vibratome (Fig. 1B). Sections were separated from the bone using a scalpel and placed on a microscope slide with the articular surface oriented towards the left (Fig. 1C–D). Solute adsorption to cracked and intact surfaces was studied on the articular surface, while the cut surface (resulting from cutting by scalpel) which was not in contact with the bath solutions acted as control (Fig. 1C–D). Fluorescence intensity images were acquired using an inverted fluorescence microscope (IX81, Olympus). Sections obtained from osteochondral explants incubated in blank culture medium were also imaged as control. To quantify the images, line-scans (which provided fluorescence intensity along straight lines) were taken at various points along the surface from the edge of the articular surface into the tissue (Fig. 1E). Five line-scans were taken per image on both intact and cracked surfaces. Background intensity was subtracted and intensity curves were averaged to give a good representation of the entire surface (Fig. 1F). The mean of all three sections from individual explants was then obtained as the overall intensity curves for each explant (represented $n = 1$). For each explant, average fluorescence intensity at the first 50 μm of the curves was determined to quantify fluorescence intensities close to the articular or cracked surfaces. Average bulk fluorescence intensity of explants was also determined using the averaged intensity curves of individual explants to compare the uptake of different solutes into the cartilage volume. Since the amount of fluorescent labels on molecules can be different from one solute to another, absolute fluorescence intensities cannot be compared directly between solutes; measured fluorescence intensities for different solutes must first be scaled. To do this, fluorescence intensity of equilibration bath solutions were measured in all experiments. Fluorescence intensity measurements in the experiments with Dex–CHO, Dex–peptide, and peptide were then scaled such that the intensity of corresponding equilibration bath in each experiment becomes equal to the intensity of Dex equilibration bath.

2.8. Quantification of cell viability

Uninjured osteochondral explants were incubated in blank culture medium (control) or culture medium containing Dex (0.28 mg/ml), Dex–CHO (0.28 mg/ml), Dex–peptide (0.18 mg/ml) or peptide (0.0085 mg/ml) for 20–22 h. Explants were then transferred to blank culture medium for 20–22 h desorption. Explants were removed from baths, their cartilage was removed from the bone and embedded in 3.5% agar (Sigma) in PBS. 100 μm thick sections were then cut perpendicular to the articular surface using a vibratome. LIVE/DEAD assay (Life Technologies) was used to quantify live and dead chondrocytes. Cartilage sections were visualized on an Olympus IX81 inverted fluorescence microscope. For each solute, three sections from three different joints were assayed.

2.9. Histological analysis

Uninjured, injured and sliced osteochondral explants were incubated in blank culture medium for 20–22 h. They were then removed from the baths, cartilage was removed from the bone and was fixed in 4% paraformaldehyde (Thermo Scientific). Fixed cartilage samples were embedded in 3.5% agar in PBS and 100 μm thick sections were cut perpendicular to the articular surface using a vibratome. Sections were stained with Alcian Blue and Safranin-O (Sigma) for GAGs. Stained sections were then washed with PBS and visualized using an inverted microscope (Axiovert 40C, Zeiss Microscopy) equipped with a Canon

Powershot A640 digital camera attached to a Zeiss MC80DX 1.0× tube adapter.

2.10. Energy dispersive X-ray spectroscopy (EDS) on scanning electron microscopy (SEM)

Osteochondral cores from three different joints were mixed and 4 explants were used randomly. Osteochondral explants were injured and incubated in blank culture medium for 20–22 h. Explants were then removed from baths and were fixed in 2% glutaraldehyde containing 0.2 M sodium cacodylate (pH 7.2) (Sigma) for 2 h and then dehydrated in progressive concentrations of ethanol (30, 50, 70, 95, 100 and 100%) [35,36]. After being air-dried for 30 h, they were mounted on an aluminum sample stub covered with adhesive carbon tabs. Samples were sputter coated with a uniform layer of gold and studied by a scanning electron microscope (JSM-840A, JEOL) equipped with energy dispersive X-ray spectroscopy [37] at 20 kV for quantitative analysis of sulfur content at cracked and intact surfaces. Because cartilage samples are not homogeneous and polished, detected signal strength in the EDS analysis may vary due to changes in height, angle relative to the detector, and absorption. These changes in signal strength might be incorrectly attributed to changes in concentration. In order to compare the sulfur content among the different samples, sulfur count was normalized to carbon count to compensate these effects. In addition, because carbon is the most abundant element in the samples (biological samples), sulfur count/carbon count approximates the sulfur concentration. It should be noted that EDS analysis is less accurate for carbon as a light element [38]. However, since the carbon content is very high in cartilage samples, possible errors in carbon count measurements do not seem to significantly affect the sulfur content comparisons between cracked and intact surfaces.

2.11. Statistical analysis

Significant differences were identified using ANOVA and Tukey's HSD test. Values are reported as mean ± SEM. Results were considered significant where $p < 0.05$.

3. Results

3.1. Solute characterization

Absorbance spectrum of Dex–CHO (Supplementary Fig. S1B) exhibited a strong peak at 223 nm not present in the absorbance spectrum of Dex (Supplementary Fig. S1A), confirming the presence of aldehyde groups [39]. Absorbance spectra of both Dex and Dex–CHO showed strong peaks at ~495 nm due to FITC molecules [40]. The degree of aldehyde substitution obtained was found to be 0.008 mmol aldehyde groups per mg of Dex–CHO using hydroxylamine titration assay. Considering the average molecular weight of glucose units of dextran and average number of hydroxyl groups in each glucose unit to be 162 and 2.5, respectively, it was found that 51.3% of hydroxyl groups were substituted with aldehyde groups.

Raman spectrum of Dex–peptide (Supplementary Fig. S1D) exhibited two moderate peaks at 750–825 and 3350–3500 cm^{-1} and a weak peak at 1700–1800 cm^{-1} not present in Raman spectrum of Dex (Supplementary Fig. S1C). In addition Raman spectrum of Dex–peptide showed a stronger peak at 520–700 cm^{-1} compared to Raman spectrum of Dex. These alterations may be attributed to tyrosine (Y), arginine (R), phenylalanine (F) (since these three amino acids are the most abundant in the structure of the peptide) and amide band [41]. The maximum possible degree of peptide conjugation to dextran was calculated to be only 5.3% (mole peptide/mole hydroxyl groups in original dextran molecules). Therefore, it is not surprising that added peaks are not strong.

3.2. Decreased solute adsorption to cracked surfaces of injured and sliced explants

Examples of fluorescence microscopy images of explants equilibrated with culture medium baths containing Dex, Dex–CHO, Dex–peptide or peptide are shown in Fig. 2A*i*–D*iii*. Strong solute accumulation at articular surfaces of uninjured explants was observed for all solutes; solute intensity deeper within the cartilage through to control edge was less intense and more uniform (Fig. 2A*i*, B*i*, C*i* and D*i*). Similarly, in injured and sliced explants intensity was uniform within the tissue and strong solute accumulation was observed at intact surfaces for all solutes. However, there was less intensity at fissure sites compared with intact surfaces and was only slightly higher than within the cartilage (Fig. 2A*ii*–*iii*, B*ii*–*iii*, C*ii* and D*ii*–*iii*). No experiment was performed with sliced explants for Dex–peptide. Quantification of fluorescence images revealed significantly lower average intensities at cracked surfaces of injured and sliced explants compared to average intensities at intact surfaces of the same explants (Fig. 2E). Average ratios of cracked surface intensity to intact surface intensity within the same explants were significantly lower than 1 for uninjured explants (ranged between 0.29 ± 0.05 and 0.46 ± 0.10) with no significant difference among solutes or injured and sliced explants (Fig. 2E).

Examples of fluorescence microscopy images taken after incubation of explants in culture medium baths containing Dex, Dex–CHO or peptide and subsequent desorption in blank culture medium are shown in Fig. 3A*i*–C*iii*. Similar to the observations after adsorption (equilibration), solute accumulation at articular surfaces of uninjured explants and intact surfaces of injured and sliced explants was observed for all solutes; solute intensity deeper within the cartilage through to control edge was less intense and more uniform. In injured and sliced explants average surface intensity at fissure sites was less intense than average intensity at intact surfaces and was only slightly higher than uniform intensity within the cartilage for all solutes (Fig. 3A*ii*–*iii*, B*ii*–*iii* and C*ii*–*iii*). The intensities were lower after desorption than after equilibration, however brightness of images were adjusted so that differential adsorption at cracked and intact surfaces are clear. Quantification of fluorescence images revealed significantly lower average intensities at cracked surfaces of injured and sliced explants compared to average intensities at intact surfaces of the same explants (Fig. 3D). Average ratios of cracked surface intensity to intact surface intensity within the same explants were significantly lower than theoretical value of 1 for uninjured explants (ranged between 0.31 ± 0.05 and 0.46 ± 0.05) with no significant difference among solutes or injured and sliced explants (Fig. 3D).

3.3. Altered solute adsorption to intact surfaces of injured and sliced explants

Average intensities at intact surfaces of injured and sliced explants were normalized to average surface intensities of uninjured (control) explants. No general trend was observed in normalized intensities at surfaces of uninjured explants and intact surfaces of injured and sliced explants between different groups (uninjured, injured and sliced) or between solutes (Fig. 2F) after explant equilibration with Dex, Dex–CHO, Dex–peptide or peptide. However, a general trend of increased average surface intensity in intact surfaces of sliced and injured explants compared with surfaces of uninjured explants was observed for explants equilibrated with Dex, Dex–CHO or peptide after subsequent desorption in blank culture medium (Fig. 3E). Increased intensities were more significant in sliced explants. These findings suggest that solute adsorption to intact surfaces of injured and sliced explants is less reversible compared with adsorption to surfaces of uninjured explants.

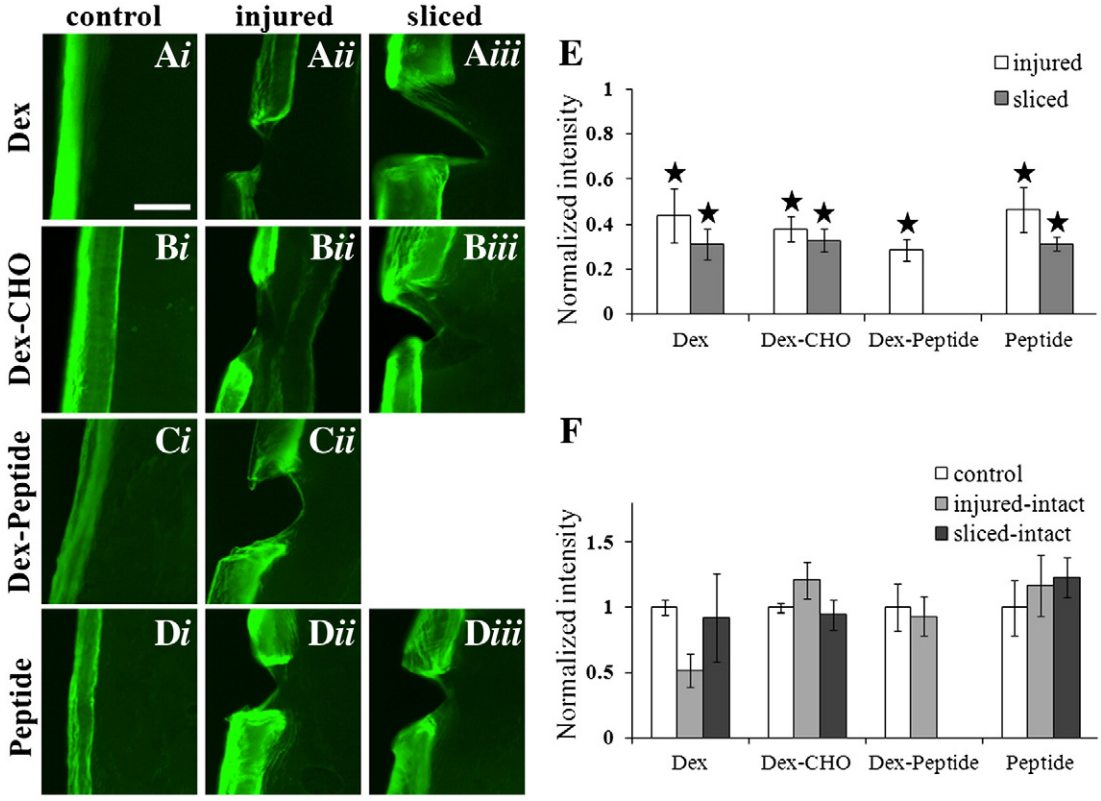

Fig. 2. Fluorescence microscope images of sections of uninjured (control) (column *i*), injured (column *ii*) and sliced (column *iii*) cartilage explants equilibrated with (A) dextran (Dex), (B) aldehyde–dextran (Dex–CHO), (C) dextran conjugated with chondroitin sulfate-binding peptide (Dex–peptide) or (D) chondroitin sulfate-binding peptide (peptide), all labeled with fluorescein isothiocyanate (FITC). (E) Mean ratio of cracked surface fluorescence intensity normalized to intact surface fluorescence intensity within individual injured and sliced explants after equilibration with solutes. Statistical comparisons were made to a ratio of 1 for uninjured explants. (F) Mean fluorescence intensity of surfaces of uninjured explants and intact surfaces of injured and sliced explants normalized to fluorescence intensity of surfaces of uninjured explants after equilibration with solutes. Scale bar is 200 μm. Mean ± SEM ($n = 4$ for uninjured Dex–CHO, $n = 6$ for all other conditions); ★: $p < 0.01$.

3.4. Increased surface adsorption and bulk uptake of dextran after chemical modifications

Absolute average intensities at surfaces of uninjured (control) explants and intact surfaces of injured and sliced explants equilibrated with Dex, Dex–CHO, Dex–peptide or peptide were compared to study the effect of chemical modifications on surface adsorption (Fig. 4A). The adsorptions of Dex–CHO and Dex–peptide were higher than adsorption of Dex, but the differences were significant only between Dex–CHO and Dex. Adsorption of Dex–peptide was lower than adsorption of Dex–CHO, but the difference was significant only for injured explants equilibrated with Dex–peptide. Dex–CHO and peptide revealed the highest adsorptions among solutes with no significant difference between them. Peptide adsorption was significantly higher than adsorption of Dex and Dex–peptide.

Absolute average intensities within uninjured (control), injured and sliced explants equilibrated with Dex, Dex–CHO, Dex–peptide or peptide were compared to study the effect of chemical modification on solute uptake (Fig. 4B). Consistent with surface adsorption, solute uptake was highest for Dex–CHO and peptide with no significant difference between them. Uptake of Dex–CHO and Dex–peptide were higher than uptake of Dex; however, the difference was significant only between uninjured and injured explants equilibrated with Dex–CHO and explants equilibrated with Dex. Uptake of Dex–CHO was higher than Dex–peptide. Differences between uninjured and injured explants equilibrated with Dex–CHO and injured explants equilibrated with Dex–peptide were significant. Peptide uptake was higher than Dex and Dex–peptide uptake with significant difference between uninjured and injured explants equilibrated with peptide and explants equilibrated with Dex and also between uninjured explants equilibrated with peptide and explants equilibrated with Dex–peptide. Consistent with previous findings [17,19], no significant difference in bulk uptakes was observed between uninjured, injured or sliced explants for each solute.

3.5. Long-term desorption

Because of weak adsorption and uptake of Dex (Fig. 4), long-term desorption experiments were performed only for Dex–CHO, Dex–peptide and peptide. For the explants equilibrated with Dex–peptide, average surface intensity dropped to 2% of its value at day 0 (equilibration in baths) after 2 days desorption; in the case of peptide, the average surface intensity dropped to zero (Fig. 5A). On the other hand, for the explants equilibrated with Dex–CHO surface intensity dropped by 56% after 2 days desorption with small decrease between days 2 and 5 (only 6% decrease) which suggests that some molecules adsorb irreversibly. Solute uptake for Dex–peptide dropped by 99% after 2 days desorption, while peptide uptake dropped to zero. Dex–CHO uptake decreased gradually by 78% from day 0 to day 5 with more rapid decrease between days 0 and 2 (54%) (Fig. 5B).

3.6. Cell viability of explants was not decreased after incubation in solutes

Incubation of uninjured explants in Dex (Fig. 6A), Dex–CHO (Fig. 6B), Dex–peptide (Fig. 6C) or peptide (Fig. 6D) baths did not decrease the cell viability. Quantified viabilities expressed as percent

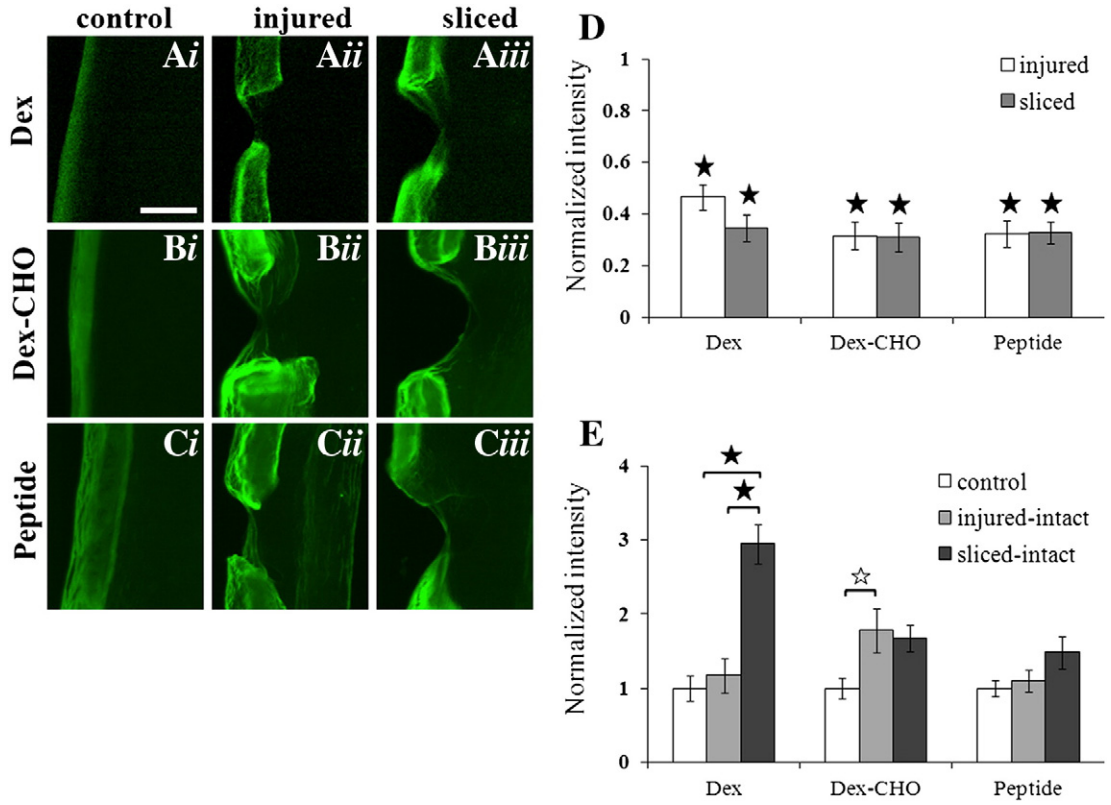

Fig. 3. Fluorescence microscope images of sections of uninjured (control) (column *i*), injured (column *ii*) and sliced (column *iii*) cartilage explants equilibrated with desorption baths of blank chondrocyte culture medium after equilibration with (A) dextran (Dex), (B) aldehyde–dextran (Dex–CHO) or (C) chondroitin sulfate-binding peptide (peptide), all labeled with fluorescein isothiocyanate (FITC). (D) Mean ratio of cracked surface fluorescence intensity normalized to intact surface fluorescence intensity within individual injured and sliced explants after equilibration with solutes and subsequent desorption. Statistical comparisons were made to a ratio of 1 for uninjured explants. (E) Mean fluorescence intensity of surfaces of uninjured explants and intact surfaces of injured and sliced explants normalized to fluorescence intensity of surfaces of uninjured explants after equilibration with solutes and subsequent desorption. Scale bar is 200 μm. Mean ± SEM (n = 6); ☆: $p < 0.05$; ★: $p < 0.01$.

of live cells were 87.1 ± 3.9% for Dex, 87.8 ± 2.9% for Dex–CHO, 78.4 ± 5.4% for Dex–peptide and 89.2 ± 3.4% for peptide with no significant difference between solutes or between solutes and control (80.3 ± 0.8%) (Fig. 6E).

3.7. Glycosaminoglycan distribution at cracked and intact surfaces of cartilage

Alcian Blue and Safranin-O staining showed lower GAG content near articular surfaces (Fig. 7A–F). While in some images of injured and sliced explants GAG content was found to be lower at cracked regions (Fig. 7E, for example), these observations were not consistent (Fig. 7B, for example). On the other hand, EDS analysis showed higher normalized sulfur content at cracked surfaces compared to intact surfaces (Fig. 7G). Since GAG molecules are highly sulfated [42], changes in GAG content may be represented by changes in sulfur composition.

4. Discussion

Observed significantly lower solute adsorptions at cracked surfaces of injured and sliced cartilage explants than intact surfaces after equilibration with solutes (Fig. 2A–E) or subsequent desorption (Fig. 3A–D) are important because they may open new avenues for development of customized imaging agents for early detection of articular cartilage surface injuries and irregularities. In addition, the findings may improve our understanding of the ultrastructure of intact and fissure surfaces of cartilage and the nature of solute–surface interactions.

The ratios of fluorescence intensity at fissure surfaces to intensity at intact surfaces of injured and sliced explants were all significantly less than 1 for uninjured explants (Figs. 2E and 3D). Differences in intensities at damaged and intact surfaces seem to be significant enough to be used for injury detection; intensity is almost uniform in intact regions of cartilage surface while spots of lower intensity may represent sites of injury. There was no significant difference in the intensity ratios between injured and sliced explants which suggests that the mechanism of differential adsorption is independent of the nature of damage. Therefore, surface fissures induced by both impact injuries or slicing can be detected by differential adsorption. Differential adsorption was also detected after a desorption process. Hence, short-term washout with synovial fluid does not limit the applicability of this technique.

The exact nature of biochemical or structural changes at fissure sites of damaged cartilage which results in altered solute–surface interactions is unknown, because the ultrastructure of the cartilage superficial surface is not fully understood [43] and solute–matrix interactions are very complex and solute-specific [44]. The superficial layer of cartilage consists of an acellular collagen-poor layer (lamina splendens, about 1 μm thick) and an underlying superficial tangential zone [5,45]. It has been reported that lamina splendens consists of two sub-zones: (i) a superficial anionic, proteinic, collagen-free layer, about 50 nm thick and poor in chondroitin and keratan sulfate and (ii) a less anionic layer, probably rich in chondroitin sulfate [5,45,46]. Almost all studies agree on the anionic nature of the articular surface of cartilage [45,47]. One study showed that cationic proteins with pIs greater than 7.0 and molecular weights larger than 40 kDa bind to articular cartilage and are retained in the joint for many days [48]. Therefore, electrostatic

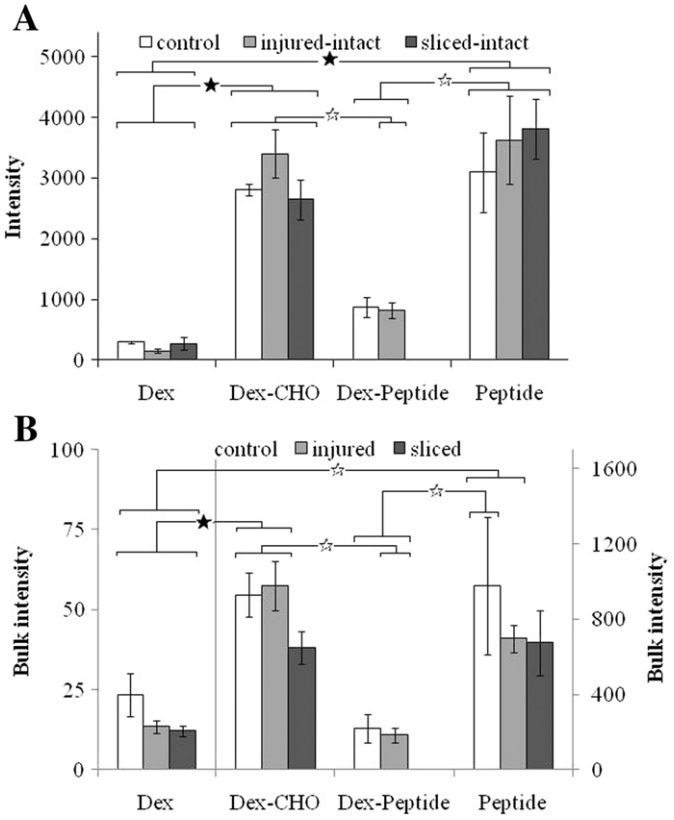

Fig. 4. (A) Average fluorescence intensity of surfaces of uninjured (control) cartilage explants and intact surfaces of injured and sliced cartilage explants and (B) average bulk fluorescence intensity of uninjured (control), injured and sliced cartilage explants equilibrated with dextran (Dex), aldehyde–dextran (Dex–CHO), dextran conjugated with chondroitin sulfate-binding peptide (Dex–peptide) or chondroitin sulfate-binding peptide (peptide), all labeled with fluorescein isothiocyanate (FITC). Mean ± SEM (n = 4 for control Dex–peptide, n = 6 for all other conditions); ☆: $p < 0.05$; ★: $p < 0.01$.

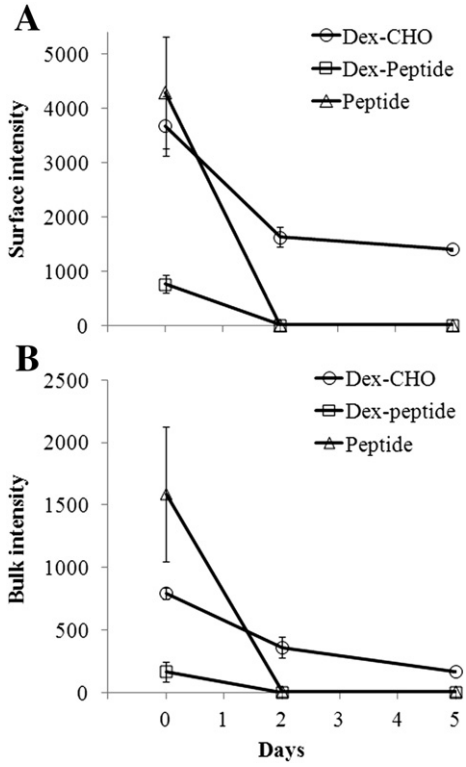

Fig. 5. Average (A) surface and (B) bulk fluorescence intensity of uninjured (control) cartilage explants equilibrated with fluorescently labeled aldehyde–dextran (Dex–CHO), dextran conjugated with chondroitin sulfate-binding peptide (Dex–peptide) or chondroitin sulfate-binding peptide (peptide) right after equilibration (day 0) and after subsequent desorption in blank chondrocyte culture medium for 2 or 5 days. Mean ± SEM (n = 3).

interactions may be responsible for the strong adsorption of solutes to intact surfaces of cartilage. Removal or disruption of the anionic layer at fissure sites can lead to decreased solute adsorption. Since this anionic layer is rich in proteins, its removal can also influence the aldehyde–amine bindings in the case of Dex–CHO. In addition, since fissures typically extended no deeper than 100–200 μm, at fissures solutes interact with the tangential superficial zone which is poor in chondroitin sulfate [49,50]. On the other hand, the concentration of chondroitin sulfate is high 50 nm below the articular surface [46]. Therefore, it is possible that decreased adsorption of Dex–peptide and peptide onto cracked surfaces is due to altered chondroitin sulfate concentration. Finally, biochemical changes at fissures due to secretion of biochemical mediators after injury [51,52] may also be involved in altered adsorption.

Due to the hydrophilic nature of GAGs and strong repulsion between their negative charges, it may be hypothesized that GAGs expand into spaces where cartilage has been cracked as the collagen network has been disrupted. The expansion of these GAGs at fissures may limit the access of other molecules to cracked surfaces and can lead to decreased adsorption. However due to expansion, GAG concentration near fissures may not be higher. This hypothesis is supported by histological staining (Fig. 7A–F) and lower adsorption of Dex–peptide and peptide to cracked surfaces (Figs. 2E and 3D). Although energy dispersive X-ray spectroscopy showed higher sulfur content at cracked surfaces (Fig. 7G), it may be because of dehydration and shrinkage of exposed GAGs.

The fact that solute adsorption was less reversible at intact surfaces of injured and sliced explants than surfaces of uninjured explants may imply structural or biochemical changes at intact surfaces of injured and sliced explants in addition to fissures. Therefore, solute adsorption to cartilage surfaces is able to detect micro-damage or biochemical changes at regions which visually look healthy. Structural and biochemical changes at intact surfaces of mechanically injured explants are expected, because impact injury may lead to micro-damage to the collagen network. However, altered properties at intact surfaces of sliced explants are not trivial and may be due to biochemical mediators secreted after slicing [51,52] or other unknown effects.

Dextran modification with aldehyde groups or the CS-binding peptide enhanced its surface adsorption and bulk uptake (Fig. 4). However, it did not affect the ratios of fissure surface intensity to intact surface intensity (Figs. 2E and 3D). Increased adsorption of modified dextrans with the same level of differential adsorption can be useful clinically since lower concentrations may be required. Increased adsorption of Dex–CHO is consistent with previous findings [28] and can be attributed to the binding of aldehyde groups to amine groups of proteins present at the superficial layer of cartilage [5,45]. Increased adsorption of Dex–peptide can be attributed to specific binding to chondroitin sulfate molecules. However since in some studies it has been reported that chondroitin sulfate is absent in the first 50 nm of the superficial layer [5,45], it may also be due to nonspecific binding to proteins or electrostatic attraction to the anionic surface of cartilage. Increased uptake of dextran after modification with aldehyde groups and the CS-binding peptide may be due to binding to proteins or chondroitin sulfate molecules, respectively, electrostatic interactions and/or decreased molecular weight of dextran after oxidation [53]. While strong adsorption can lead to more sensitive imaging, adsorption needs to be reversible to be clinically applicable. In contrast with Dex–peptide and peptide, adsorption and uptake of Dex–CHO were not reversible (Fig. 5) which may limit its clinical application.

Dex–peptide seemed to be the best choice among the solutes studied as potential carrier molecules. Like other solutes, Dex–peptide showed differential adsorption and did not decrease the cell viability.

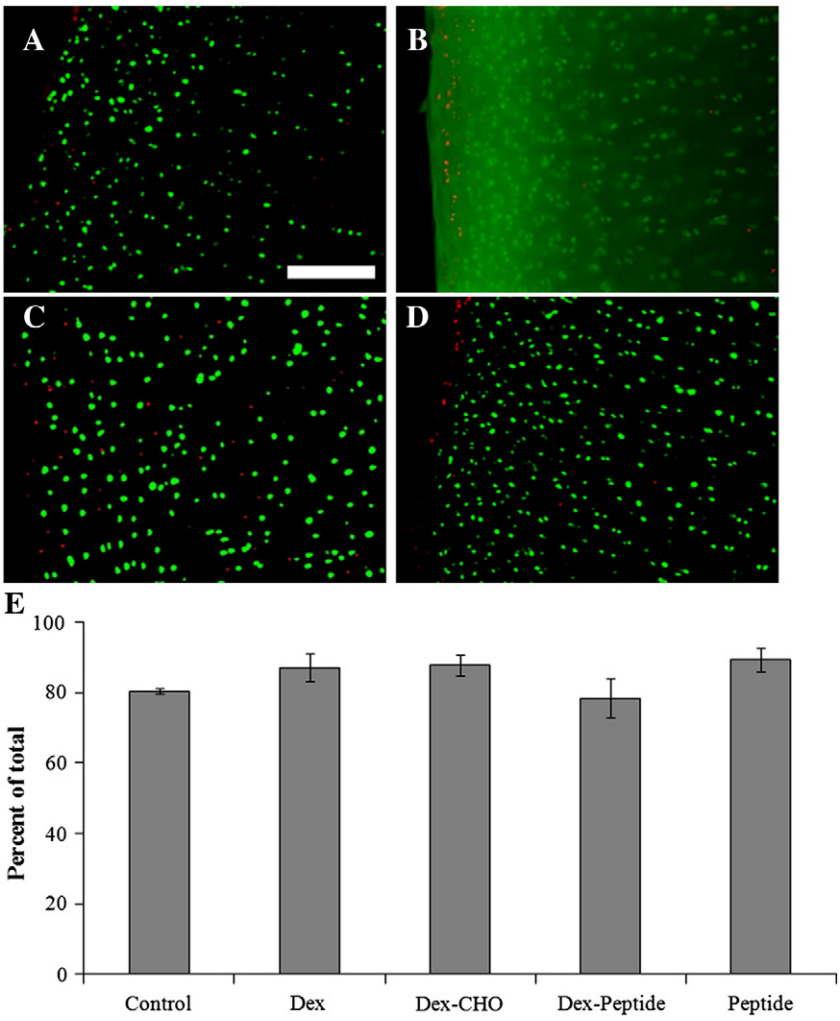

Fig. 6. Fluorescence microscope images of LIVE/DEAD assays of 200 μm thick sections of uninjured cartilage explants. Explants were equilibrated with (A) dextran, (B) aldehyde–dextran, (C) dextran conjugated with chondroitin sulfate-binding peptide, (D) chondroitin sulfate-binding peptide or blank chondrocyte culture medium (control) and subsequently with blank chondrocyte culture medium desorption baths before LIVE/DEAD assay. Scale bar is 200 μm. (E) Viable (green) chondrocytes were quantified as a percentage of total cells. Mean ± SEM (n = 3).

On the other hand, its adsorption was stronger than dextran (but still reversible) and it is easy to conjugate MRI or CT contrast agents to its dextran backbone. Peptide had all of these benefits, but it might be more difficult to conjugate contrast agents to a peptide.

In this study, all the studied solutes were conjugated with FITC. It has been previously shown that fluorescent labeling of solutes can affect their adsorption to cartilage surfaces [18]. Therefore, while altered adsorption of dextran after modification with the peptide and aldehyde groups

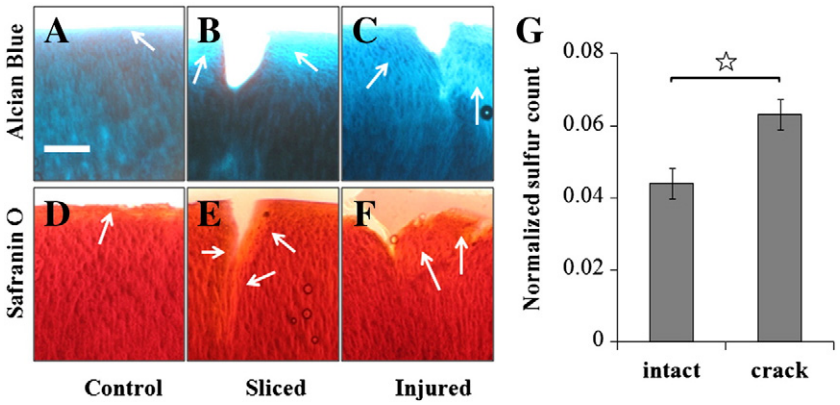

Fig. 7. Alcian Blue (A–C) and Safranin-O (D–F) histological staining of 200 μm thick sections of uninjured (control) (A and D), sliced (B and E) and injured (C and F) cartilage explants. Arrows show regions with lower glycosaminoglycan content. Scale bar is 200 μm. (G) Mean sulfur count at intact and cracked surfaces of injured cartilage explants normalized to carbon count obtained by scanning electron microscopy (SEM) with energy-dispersive X-ray spectroscopy (EDS) analysis. Mean ± SEM (n = 4); ☆: $p < 0.05$.

suggests that these molecules are involved in the adsorption mechanism, conjugated FITC molecules may also have some contribution to the observed adsorption behavior. However, the effect of fluorescent labeling is likely minimized in this study, as it has been shown that interactions of solutes with cartilage are less affected when conjugated by FITC compared with positively charged fluorophores (TRITC and TAMRA) [18]. Future studies using radioactive solutes or solutes conjugated with CT or MRI contrast agents can further investigate the individual role of studied solutes and fluorescent labels.

5. Conclusions

The findings of the present study may open new avenues for development of customized imaging tools based on solute adsorption to cartilage surfaces. This approach has the advantage that surface injuries and abnormalities can be detected before surface damage leads to structural or biochemical changes in the tissue volume. Moreover, this technique may be able to detect micro-damage or biochemical changes at regions which visually look healthy in addition to fissures. FITC labeled dextran, dextran conjugated with a chondroitin sulfate (CS)-binding peptide and the CS-binding peptide alone showed promising results for potential use as carrier molecules which can be conjugated with CT or MRI contrast agents to develop cartilage-specific contrast agents. Moreover, they can be used directly in in vivo fluorescent imaging methods [54].

Supplementary data to this article can be found online at http://dx.doi.org/10.1016/j.bbagen.2013.10.022.

Conflict of interest

The authors have no conflict of interest.

Acknowledgements

This study was supported by the Canada Research Chair and NSERC Discovery Grant programs. We thank Ranjan Roy and Andrew Golsztajn for their technical help in the experiments.

References

[1] S.S. Chen, Y.H. Falcovitz, R. Schneiderman, A. Maroudas, R.L. Sah, Depth-dependent compressive properties of normal aged human femoral head articular cartilage: relationship to fixed charge density, Osteoarthr. Cartil. 9 (2001) 561–569.
[2] J.-K. Suh, S. Scherping, T. Mardi, J. Richard Steadman, S.L.Y. Woo, Basic science of articular cartilage injury and repair, Oper. Tech. Sports Med. 3 (1995) 78–86.
[3] H.J. Mankin, Localization of tritiated thymidine in articular cartilage of rabbits III. Mature articular cartilage, J. Bone Joint Surg. Am. 45 (1963) 529–540.
[4] I. Sulzbacher, Osteoarthritis: histology and pathogenesis, Wien. Med. Wochenschr. 163 (2013) 212–219.
[5] P. Kumar, M. Oka, J. Toguchida, M. Kobayashi, E. Uchida, T. Nakamura, K. Tanaka, Role of uppermost superficial surface layer of articular cartilage in the lubrication mechanism of joints, J. Anat. 199 (2001) 241–250.
[6] M.A. Davis, W.H. Ettinger, J.M. Neuhaus, S.A. Cho, W.W. Hauck, The association of knee injury and obesity with unilateral and bilateral osteoarthritis of the knee, Am. J. Epidemiol. 130 (1989) 278–288.
[7] T.R. McCauley, D.G. Disler, MR imaging of articular cartilage, Radiology 209 (1998) 629–640.
[8] P.N. Bansal, N.S. Joshi, V. Entezari, B.C. Malone, R.C. Stewart, B.D. Snyder, M.W. Grinstaff, Cationic contrast agents improve quantification of glycosaminoglycan (GAG) content by contrast enhanced CT imaging of cartilage, J. Orthop. Res. 29 (2011) 704–709.
[9] C.W. Hayes, W.F. Conway, Evaluation of articular cartilage: radiographic and cross-sectional imaging techniques, Radiographics 12 (1992) 409–428.
[10] A.S. Kallioniemi, J.S. Jurvelin, M.T. Nieminen, M.J. Lammi, J. Töyräs, Contrast agent enhanced pQCT of articular cartilage, Phys. Med. Biol. 52 (2007) 1209.
[11] P.N. Bansal, N.S. Joshi, V. Entezari, M.W. Grinstaff, B.D. Snyder, Contrast enhanced computed tomography can predict the glycosaminoglycan content and biomechanical properties of articular cartilage, Osteoarthr. Cartil. 18 (2010) 184–191.
[12] A. Bashir, M.L. Gray, R.D. Boutin, D. Burstein, Glycosaminoglycan in articular cartilage: in vivo assessment with delayed Gd(DTPA)(2−)-enhanced MR imaging, Radiology 205 (1997) 551–558.
[13] A.W. Palmer, R.E. Guldberg, M.E. Levenston, Analysis of cartilage matrix fixed charge density and three-dimensional morphology via contrast-enhanced microcomputed tomography, Proc. Natl. Acad. Sci. 103 (2006) 19255–19260.
[14] P.N. Bansal, R.C. Stewart, V. Entezari, B.D. Snyder, M.W. Grinstaff, Contrast agent electrostatic attraction rather than repulsion to glycosaminoglycans affords a greater contrast uptake ratio and improved quantitative CT imaging in cartilage, Osteoarthr. Cartil. 19 (2011) 970–976.
[15] H.T. Kokkonen, J.S. Jurvelin, V. Tiitu, J. Töyräs, Detection of mechanical injury of articular cartilage using contrast enhanced computed tomography, Osteoarthr. Cartil. 19 (2011) 295–301.
[16] T.S. Silvast, J.S. Jurvelin, V. Tiitu, T.M. Quinn, J. Töyräs, Bath concentration of anionic contrast agents does not affect their diffusion and distribution in articular cartilage in vitro, Cartilage 4 (2013) 42–51.
[17] H.C. Chin, M. Moeini, T.M. Quinn, Solute transport across the articular surface of injured cartilage, Arch. Biochem. Biophys. 535 (2013) 241–247.
[18] M. Moeini, T.M. Quinn, Solute adsorption to surfaces of articular cartilage explants: apparent versus actual partition coefficients, Soft Matter 8 (2012) 11880–11888.
[19] S.G.A. Decker, M. Moeini, H.C. Chin, D.H. Rosenzweig, T.M. Quinn, Adsorption and distribution of fluorescent solutes near the articular surface of mechanically injured cartilage, Biophys. J. 105 (2013) 1–10.
[20] C.E. Odya, Y. Levin, E.G. Erdös, C.J.G. Robinson, Soluble dextran complexes of kallikrein, bradykinin and enzyme inhibitors, Biochem. Pharmacol. 27 (1978) 173–179.
[21] S. Penugonda, A. Kumar, H.K. Agarwal, K. Parang, R. Mehvar, Synthesis and in vitro characterization of novel dextran–methylprednisolone conjugates with peptide linkers: effects of linker length on hydrolytic and enzymatic release of methyl-prednisolone and its peptidyl intermediates, J. Pharm. Sci. 97 (2008) 2649–2664.
[22] C. Larsen, Dextran prodrugs — structure and stability in relation to therapeutic activity, Adv. Drug Deliv. Rev. 3 (1989) 103–154.
[23] R. Mehvar, Dextrans for targeted and sustained delivery of therapeutic and imaging agents, J. Control. Release 69 (2000) 1–25.
[24] Y. Chau, F.E. Tan, R. Langer, Synthesis and characterization of dextran–peptide–methotrexate conjugates for tumor targeting via mediation by matrix metalloproteinase II and matrix metalloproteinase IX, Bioconjug. Chem. 15 (2004) 931–941.
[25] L. Molteni, Dextran and inulin conjugates as drug carriers, in: K.J. Widder, R. Green (Eds.), Methods in Enzymology, vol. 112, Academic Press, 1985, pp. 285–298.
[26] Z.A. Rogovin, A.D. Vernik, K.P. Khomiakov, O.P. Laletina, M.A. Penenzhik, Study of the synthesis of dextran derivatives, J. Macromol. Sci. Chem. 6 (1972) 569–593.
[27] E. Schacht, J. Vermeersch, F. Vandoorne, R. Vercauteren, J.P. Remon, Synthesis and characterization of some modified polysaccharides containing drug moieties, J. Control. Release 2 (1985) 245–256.
[28] K. Chawla, H.O. Ham, T. Nguyen, P.B. Messersmith, Molecular resurfacing of cartilage with proteoglycan 4, Acta Biomater. 6 (2010) 3388–3394.
[29] S. Maeda, T. Miyabayashi, J.K. Yamamoto, G.D. Roberts, A.J. Lepine, R.M. Clemmons, Temporal dynamic changes in synthesis of chondroitin sulfate isomers in canine articular chondrocyte culture, J. Vet. Med. Sci. 65 (2003) 1373–1376.
[30] J.M.G. Reyes, S. Herretes, A. Pirouzmanesh, D.-A. Wang, J.H. Elisseeff, A. Jun, P.J. McDonnell, R.S. Chuck, A. Behrens, A modified chondroitin sulfate aldehyde adhesive for sealing corneal incisions, Invest. Ophthalmol. Vis. Sci. 46 (2005) 1247–1250.
[31] K.C. Butterfield, A. Conovaloff, M. Caplan, A. Panitch, Chondroitin sulfate-binding peptides block chondroitin 6-sulfate inhibition of cortical neurite growth, Neurosci. Lett. 478 (2010) 82–87.
[32] S.C. Tam, J. Blumenstein, J.T. Wong, Soluble dextran–hemoglobin complex as a potential blood substitute, Proc. Natl. Acad. Sci. 73 (1976) 2128–2131.
[33] H. Zhao, N. Heindel, Determination of degree of substitution of formyl groups in polyaldehyde dextran by the hydroxylamine hydrochloride method, Pharm. Res. 8 (1991) 400–402.
[34] V. Morel, T.M. Quinn, Cartilage injury by ramp compression near the gel diffusion rate, J. Orthop. Res. 22 (2004) 145–151.
[35] B. Arborgh, P. Bell, U. Brunk, V. Collins, The osmotic effect of glutaraldehyde during fixation. A transmission electron microscopy, scanning electron microscopy and cytochemical study, J. Ultrastruct. Res. 56 (1976) 339.
[36] F. Ghadially, R. Ailsby, A. Oryschak, Scanning electron microscopy of superficial defects in articular cartilage, Ann. Rheum. Dis. 33 (1974) 327.
[37] N.B. Kavukcuoglu, Q. Li, N. Pleshko, J. Uitto, Connective tissue mineralization in *Abcc6*$^{-/-}$ mice, a model for pseudoxanthoma elasticum, Matrix Biol. 31 (2012) 246–252.
[38] J.I. Goldstein, D.E. Newbury, D.C. Joy, P. Echlin, C.E. Lyman, E. Lifshin, L. Sawyer, J.R. Michael, Scanning Electron Microscopy and X-ray Microanalysis, Third ed. Kluwer Academic/Plenum Publishers, New York, 2003.
[39] G.D. Christian, Analytical chemistry, 6th ed. Wiley India Pvt. Limited, 2007.
[40] I.D. Johnson, The Molecular Probes Handbook: a Guide to Fluorescent Probes and Labeling Technologies, 11th ed. Life Technologies Corporation, Carlsbad, CA, 2010.
[41] R. Tuma, Raman spectroscopy of proteins: from peptides to large assemblies, J. Raman Spectrosc. 36 (2005) 307–319.
[42] A. Maroudas, Transport of solutes through cartilage: permeability to large molecules, J. Anat. 122 (1976) 335–347.
[43] R.V. Patel, J.J. Mao, Microstructural and elastic properties of the extracellular matrices of the superficial zone of neonatal articular cartilage by atomic force microscopy, Front. Biosci. 8 (2003) a18–a25.
[44] M. Moeini, K.-B. Lee, T.M. Quinn, Temperature affects transport of polysaccharides and proteins in articular cartilage explants, J. Biomech. 45 (2012) 1916–1923.
[45] C.R. Orford, D.L. Gardner, Ultrastructural histochemistry of the surface lamina of normal articular cartilage, Histochem. J. 17 (1985) 223–233.
[46] M. Uesugi, H.E. Jasin, Macromolecular transport across the superficial layer of articular cartilage, Osteoarthr. Cartil. 8 (2000) 13–16.

[47] R. Stanescu, S.J. Leibovich, The negative charge of articular cartilage surfaces. An electron microscopic study using cationized ferritin, J. Bone Joint Surg. Am. 64 (1982) 388–398.
[48] P.L.v. Lent, W.B.v.d. Berg, J. Schalkwijk, L.B.v.d. Putte, L.v.d. Bersselaar, The impact of protein size and charge on its retention in articular cartilage, J. Rheumatol. 14 (1987) 798–805.
[49] H. Muir, P. Bullough, A. Maroudas, The distribution of collagen in human articular cartilage with some of its physiological implications, J. Bone Joint Surg. Br. 52-B (1970) 554–563.
[50] B.L. Schumacher, J.A. Block, T.M. Schmid, M.B. Aydelotte, K.E. Kuettner, A novel proteoglycan synthesized and secreted by chondrocytes of the superficial zone of articular cartilage, Arch. Biochem. Biophys. 311 (1994) 144–152.
[51] V. Morel, T.M. Quinn, Short-term changes in cell and matrix damage following mechanical injury of articular cartilage explants and modelling of microphysical mediators, Biorheology 41 (2004) 509–519.
[52] D.H. Rosenzweig, M.J. Djap, S.J. Ou, T.M. Quinn, Mechanical injury of bovine cartilage explants induces depth-dependent, transient changes in MAP kinase activity associated with apoptosis, Osteoarthr. Cartil. 20 (2012) 1591–1602.
[53] T. Azzam, H. Eliyahu, L. Shapira, M. Linial, Y. Barenholz, A.J. Domb, Polysaccharide–oligoamine based conjugates for gene delivery, J. Med. Chem. 45 (2002) 1817–1824.
[54] G.A. Wagnieres, W.M. Star, B.C. Wilson, In vivo fluorescence spectroscopy and imaging for oncological applications, Photochem. Photobiol. 68 (1998) 603–632.